PERGAMON Journal of the Franklin Institute 337 (2000) 251–265

Journal of The Franklin Institute

www.elsevier.nl/locate/jfranklin

Chua's circuit decomposition: a systematic design approach for chaotic oscillators

A.S. Elwakil*, M.P. Kennedy

Department of Electronic and Electrical Engineering, Faculty of Engineering, University College Dublin, Belfield, Dublin 4, Ireland

Received 3 June 1999; received in revised form 23 February 2000

Abstract

The fact that Chua's circuit can be physically decomposed into a sinusoidal oscillator coupled to an active voltage-controlled nonlinear resistor is demonstrated. The sinusoidal oscillator is the beating heart of Chua's circuit and many novel implementations can be obtained by using different sinusoidal oscillator engines. In particular, inductorless realizations can be derived not by replacing the passive inductor in the classical Chua's circuit configuration with an active RC emulation, but rather by replacing the passive LC tank resonator by a sinusoidal oscillator. We provide several circuit-design examples and verify our results experimentally. Finally, we state a conjecture which we believe forms a basis for the design of autonomous analog chaotic oscillators. © 2000 The Franklin Institute. Published by Elsevier Science Ltd. All rights reserved.

1. Introduction

Until recently, very few chaotic oscillators existed in the literature. This was a consequence of the fact that it was not clear how such strongly nonlinear circuits could be designed to produce chaos. In fact, many circuit designers had doubts about the possibility of designing robust chaotic oscillators. These doubts were supported by observing the reported chaotic oscillators which were either emulating a set of mathematical equations that are known to be chaotic, such as the Van der Pol, Lorenz and Mackey-Glass systems [1–3] or were intuitively discovered, such as Chua and Saito's oscillators [4–6]. Although detailed studies of the nonlinear dynamics governing these oscillators have been carried out, much less effort has been devoted to

* Corresponding author. Tel.: + 353-706-7777; fax: + 353-283-0921.

E-mail address: elwakil@nebula.ucd.ie (A.S. Elwakil).

PII: S0016-0032(00)00019-3

developing circuit-design methodologies [7]. A starting point for a design process did not seem to exist. Hence, more circuit-design-oriented studies have been carried out.

The objective of these studies is to establish methods for generating a chaotic signal with prescribed statistical properties from an electronic circuit that satisfies a set of design constraints. Such constraints may include the type of active devices used, the type and location of energy storage elements, active or passive nonlinearities, current or voltage signal processing, as well as frequency response, supply voltage and power dissipation requirements. Although statistical measures that can characterize a chaotic signal generated by an analog circuit as being suitable for a certain application are still lacking,[1] this work aims to propose a solid basis for designing analog chaotic oscillators with prescribed *circuit* requirements.

We demonstrate here that Chua's circuit can be physically decomposed into a sinusoidal oscillator coupled to a voltage-controlled nonlinear resistor. In particular, the passive *LC* tank resonator can be replaced by a general second-order sinusoidal oscillator, such as the Wien-bridge oscillator, or even a third-order one, such as the Twin-T oscillator. In this way, inductorless realizations can be obtained without using *RC* emulations of the inductor, as was done in [8–10]. We have recently performed a similar decomposition [11] of Saito's double-screw hysteresis oscillator [6], which employs a current-controlled nonlinear resistor. Our work on decomposing Chua's and Saito's classical chaotic oscillators was motivated by the observation of chaos in the Colpitts oscillator [12] and the large number of chaotic oscillators that have been introduced thereafter [13–18]. The common feature of these oscillators is that they all use a sinusoidal oscillator engine. However, the chaotic oscillators reported in [14–18] use a simple passive nonlinearity (diode or diode-connected transistor) instead of an active one, by contrast with Chua's and Saito's circuits. This should not be surprising, since there is no need for more than one energy source in the circuit. Therefore, an active nonlinear element is not necessary for chaos generation. The task of being able to design a chaotic oscillator with predefined circuit requirements is greatly simplified if only passive nonlinear devices are used since it is then sufficient to introduce any desired feature of the chaotic oscillator into its core sinusoidal (relaxation) oscillator [19]. We have proposed *diode-inductor* and *FET-capacitor* composites to permit classical sinusoidal oscillators to behave chaotically [20].

In this work, new realizations of Chua's circuit based on Wien-bridge and Twin-T sinusoidal oscillators are proposed. We present a conjecture and make clear that chaotic behavior is not associated with individual elements but rather with general circuit-independent functional blocks. PSpice simulations, numerical simulations of the derived models, and experimental results are shown.

2. Design concept

From a design-oriented point of view, understanding the behavior of a complicated circuit can be achieved by decomposing it into functional blocks. This decomposition

[1] Techniques are available to design discrete-time chaotic oscillators with prescribed statistical properties.

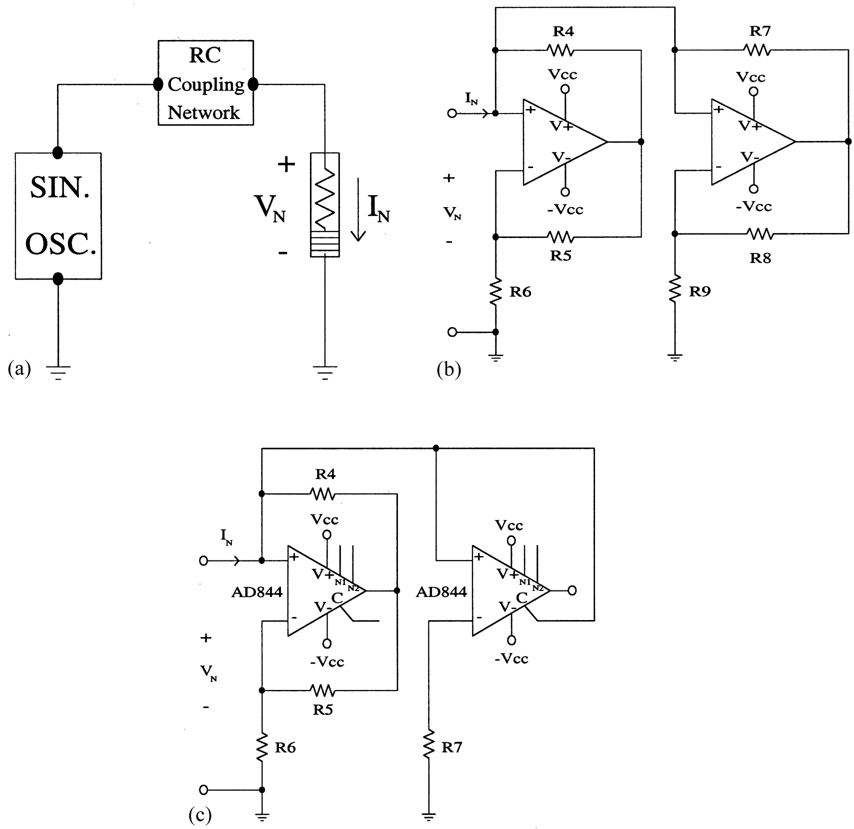

Fig. 1. (a) General configuration for producing chaos. (b) Chua's diode implementation using VOAs. (c) Using CFOAs.

process should continue until blocks with clearly defined functions and corresponding design procedures are obtained.

2.1. Chua's circuit

Consider the configuration shown in Fig. 1(a) where a general sinusoidal oscillator is coupled to a voltage-controlled nonlinear resistor via a passive *RC* network. Since there should exist at least one energy source in the configuration, at least one of these two blocks must be active. A simple *LC* tank resonator can be considered as a passive sinusoidal oscillator since oscillations which start due to arbitrary initial conditions can be sustained only if an external energy source is present. Therefore, the classical *LC–R* sinusoidal oscillator is obtained by adding a negative resistor to the tank circuit. Of course, without additional amplitude control circuitry, the nonlinearity of the active devices which are used to implement the negative resistor will tend to limit the amplitude of oscillation in practice.

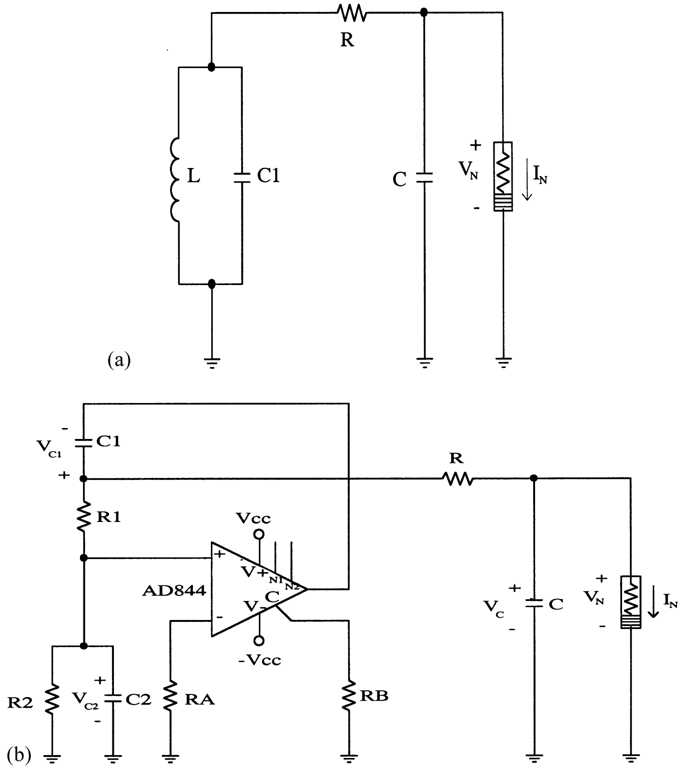

Fig. 2. (a) Classical Chua's circuit configuration. (b) Realization of Fig. 1(a) using a Wien-bridge oscillator.

Whereas a two-terminal diode is a simple passive voltage-controlled nonlinear resistor, Chua's diode is an example of an active one. Fig. 1(b) represents a standard design of this active nonlinear resistor using voltage op amps (VOAs) [7] while Fig. 1(c) is a new design using current feedback op amps (CFOAs).

Since the switching action of a nonmonotone voltage-controlled resistor depends on the voltage across its terminals, a transit capacitor must be included to complete the model [21]. This capacitor can either be an explicit or a parasitic one. The circuit in Fig. 2(a) can thus be derived from the configuration of Fig. 1(a) by using the passive LC_1 tank to replace the sinusoidal oscillator and implementing the nonlinear resistor by means of the circuits shown in Fig. 1(b) or (c). This circuit represents the well-known Chua's circuit. Indeed, realizations of this circuit reported in [5,7–10] have chosen a value for C which is 10 times smaller than the value of C_1. We will show here that even smaller ratios can preserve the double-scroll dynamics.

2.2. Implementations based on the Wien-bridge oscillator

In this section, the possibility of using an active sinusoidal oscillator instead of the passive resonator is investigated. The popular second-order Wien-bridge oscillator is chosen instead of the LC_1 tank and the resulting circuit is shown in Fig. 2(b). Here, the Wien oscillator is implemented using a CFOA configured as a noninverting voltage-controlled voltage source (VCVS) with gain $K = R_B/R_A$.

The configuration of Fig. 2(b) can be described by the following set of equations:

$$C_1 \dot{V}_{C_1} = \frac{V_C - V_{C_1} - KV_{C_2}}{R} - \frac{V_{C_1} + (K-1)V_{C_2}}{R_1}, \tag{1a}$$

$$C_2 \dot{V}_{C_2} = \frac{V_{C_1} + (K-1)V_{C_2}}{R_1} - \frac{V_{C_2}}{R_2}, \tag{1b}$$

$$C\dot{V}_C = -\frac{V_C - V_{C_1} - KV_{C_2}}{R} - I_N, \tag{1c}$$

where I_N is the current in the voltage-controlled nonlinear resistor which is modelled by

$$I_N = f(V_N) = G_b V_N + 0.5(G_a - G_b)(|V_N + V_{BP}| - |V_N - V_{BP}|), \tag{2}$$

where G_a and G_b are the slopes of the I–V characteristic in the inner and outer segments, respectively, and $\pm V_{BP}$ are the break points.

Simulations of Fig. 2(b) using PSpice[2] were performed with the Chua's diode implementation shown in Fig. 1(b) and taking: $C_1 = C_2 = C_0 = 50$ nF, $R_1 = R_2 = R_0 = 200\ \Omega$, $R_A = 1$ kΩ, $R_B = 3.4$ kΩ, $R = 1.5$ kΩ, $C = 1.5$ nF, $R_4 = 3.3$ kΩ, $R_5 = R_6 = 22$ kΩ, $R_7 = 2.2$ kΩ, $R_8 = R_9 = 220\ \Omega$ and using TL082 op amps biased with ± 9 V supplies. The resulting V_{C_1}–V_C double-scroll attractor is shown in Fig. 3(a).

Note that the theoretical gain required to start oscillations in a Wien oscillator with the *equal-R* ($R_1 = R_2 = R_0$) *equal-C* ($C_1 = C_2 = C_0$) design is $K = 3$. Hence, chaotic behavior requires K to be increased slightly beyond this nominal value ($K = 3.4$ in our PSpice simulations). It is clear that the best tuning parameter (bifurcation parameter) for the whole circuit is the gain K; this parameter can be varied by adjusting a single tunable grounded resistor (R_A or R_B). Simulations have also been performed with a switching capacitor C as small as 10 pF to confirm that it can be a parasitic capacitor. The double-scroll attractor was preserved with this value of C and with the coupling resistor R adjusted to 1.7 kΩ. Smaller values of this capacitor simply result in faster switching between the upper and lower scroll surfaces.

By introducing the following variables: $\tau = t/R_0C_0$, $X = V_{C_1}/V_{BP}$, $Y = V_{C_2}/V_{BP}$, $Z = V_C/V_{BP}$, $\varepsilon_r = R_0/R$, $\varepsilon_c = C/C_0$, $\alpha_1 = G_bR_0$ and $\alpha_2 = 0.5(G_a - G_b)R_0$, the set of equations (1) and (2) can be transformed into dimensionless form as follows:

$$\dot{X} = (1 - K - \varepsilon_r K)Y - (1 + \varepsilon_r)X + \varepsilon_r Z, \tag{3a}$$

$$\dot{Y} = X + (K-2)Y, \tag{3b}$$

[2] The simulation period is 10 ms and the step ceiling is 500 ns.

$$\varepsilon_c \dot{Z} = \varepsilon_r(X + KY - Z) - f(Z) \tag{3c}$$

and

$$f(Z) = \alpha_1 Z + \alpha_2(|Z+1| - |Z-1|). \tag{3d}$$

Numerical integration of the above system of equations was carried out using a fourth-order Runge–Kutta algorithm with a 0.001 time step and setting: $K = 3.25$, $\varepsilon_r = \frac{1}{6}$, $\varepsilon_c = 0.06$, $\alpha_1 = 0.8$ and $\alpha_2 = -0.5$. The resulting double-scroll attractor in the X–Y–Z coordinate system is shown in Fig. 3(b). With ε_c as small as 0.001 and with $K = 3.2$, the double-scroll could still be observed.

Note that when $\varepsilon_r = 0$ (no coupling), the describing equations of the Wien oscillator in the X–Y plane can be retrieved. Note also that the ratio $\varepsilon_r/\varepsilon_c$ is equal to ω_{sw}/ω_{osc} where $\omega_{sw} = 1/RC$ is proportional to the average switching frequency between the upper and lower scrolls and ω_{osc} is the sinusoidal oscillator's center frequency $(1/R_0C_0)$. For constant values of α_1 and α_2, which imply fixed nonlinear resistor parameters, (3a)–(3d) is a three-parameter $(K, \varepsilon_r, \varepsilon_c)$ system.

Note that the function performed by the switching capacitor C in Fig. 2(b) (also in Fig. 2(a)) can be maintained if it is placed in parallel with the coupling resistor R instead of directly across the nonlinear resistor. In this case, the circuit is described by

$$C_1 \dot{V}_{C_1} = -\frac{V_{C_1} + (K-1)V_{C_2}}{R_1} - I_N, \tag{4a}$$

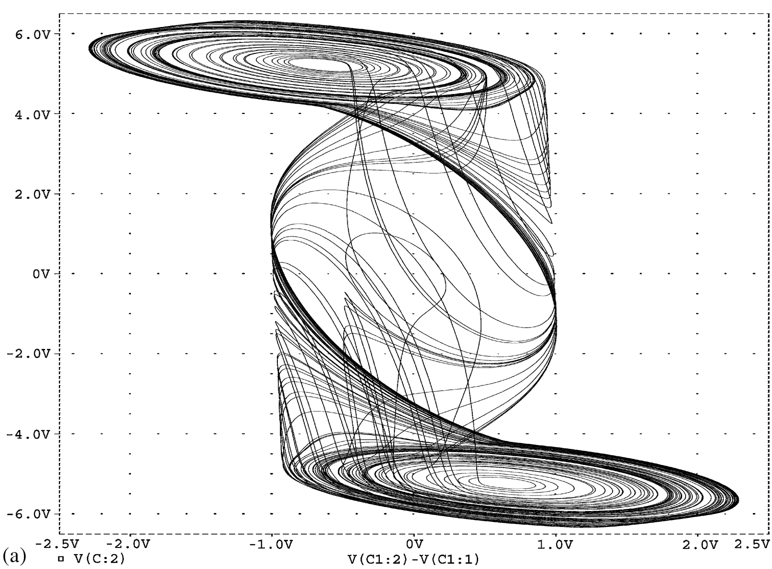

Fig. 3. (a) PSpice simulation of Fig. 2(b) demonstrating the V_{C_1}–V_C projection. (b) X–Y–Z double-scroll attractor obtained by numerical integration of (3). (c) The X–Z trajectory obtained by numerically integrating (5).

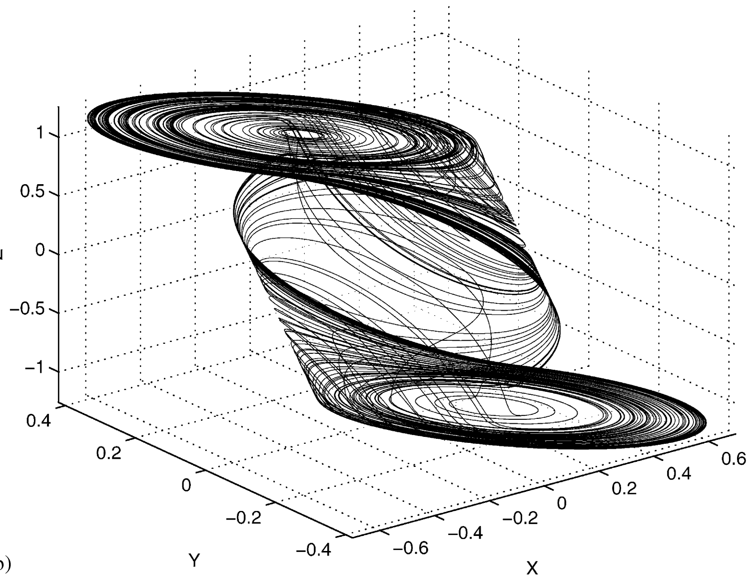

(b)

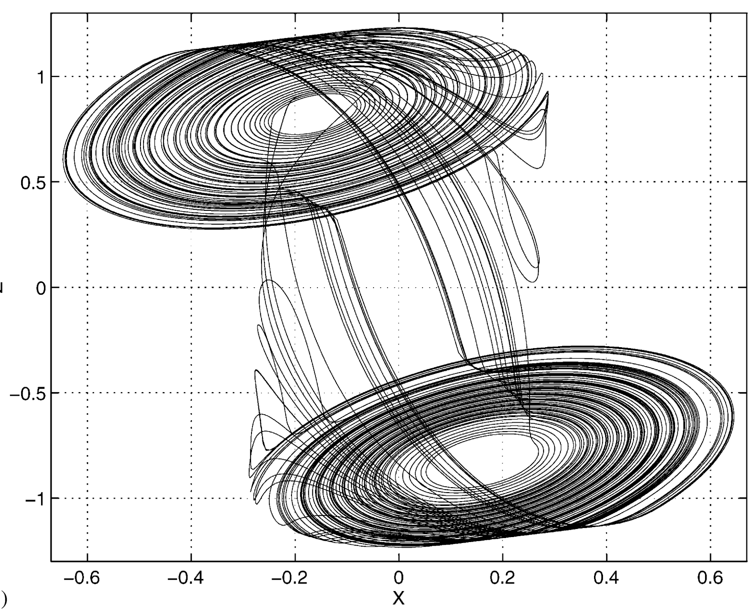

(c)

Fig. 3. (*continued*).

$$C_2\dot{V}_{C_2} = \frac{V_{C_1} + (K-1)V_{C_2}}{R_1} - \frac{V_{C_2}}{R_2}, \tag{4b}$$

$$C\dot{V}_C = -\frac{V_C}{R} - I_N \tag{4c}$$

and I_N is as given by (2) with $V_N = V_{C_1} + KV_{C_2} + V_C$.

With the same settings used above, (4) is transformed to the following dimensionless form:

$$-\dot{X} = X + (K-1)Y + f(W), \tag{5a}$$

$$\dot{Y} = X + (K-2)Y, \tag{5b}$$

$$-\varepsilon_c\dot{Z} = \varepsilon_r Z + f(W), \tag{5c}$$

where $f(W)$ has the same form as $f(Z)$ in (3d) and $W = X + KY + Z$.

Numerical integration of the above equations was performed with the same values of K, ε_c, ε_r, α_1 and α_2 used to integrate (3). An X–Z projection of the resulting trajectory is shown in Fig. 3(c).

Note that there is another internal node in the Wien-bridge oscillator to which the coupling resistor R can be connected, namely across the parallel R_2C_2 network (see Fig. 2(b)). Similar results can be obtained when coupling is made to this node and two different sets of equations corresponding to the two positions of the switching capacitor can be derived.

It should be clear that the double-scroll dynamics are associated with the functions performed by the sinusoidal oscillator and the voltage-controlled nonlinear resistor rather than with individual circuit components. This inspires numerous implementations of Chua's circuit which can be obtained by replacing the sinusoidal oscillator engine with a different one. Of course, for every different engine, new features might be obtained, as demonstrated in the next section.

2.3. Implementation based on the Twin-T oscillator

It is known that a minimum-component RC sinusoidal oscillator contains just two resistors and two capacitors. Thus, most sinusoidal oscillators are of second order. The Twin-T oscillator is one of the very few third-order sinusoidal oscillators that are known.

An implementation of the general configuration of Fig. 1(a) using the Twin-T oscillator is shown in Fig. 4(a). Here, the op amp is employed as a VCVS with gain $K = 1 + R_B/R_A$. The choice of a symmetrical Twin-T implies that $R_1 = R_2 = 2R_3 = R_0$ and $C_1 = C_2 = C_3/2 = C_0$ and the theoretical gain required to start oscillations is given by $K = 1$. Note that the voltage op amp (VOA) can be replaced directly by a CFOA as in Fig. 2(b). Similarly, the switching capacitor can be placed either across the nonlinear resistor or the coupling resistor, as shown in Fig. 4(a), which is described by the following fourth-order system of equations:

$$C_1 \dot{V}_{C_1} = C_2 \dot{V}_{C_2} - \frac{(1-K)V_{C_1} - KV_{C_2}}{R_3}, \tag{6a}$$

$$C_2 \dot{V}_{C_2} = \frac{(K-1)(V_{C_1} + V_{C_2}) + V_{C_3}}{R_2}, \tag{6b}$$

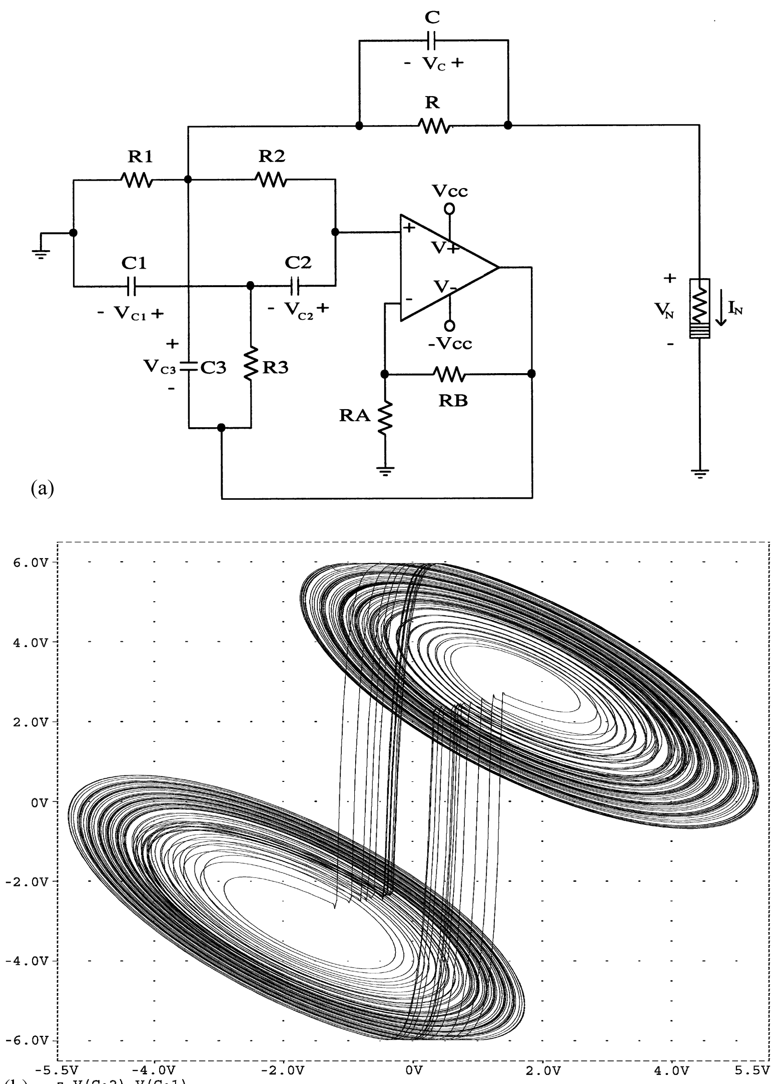

Fig. 4. (a) Twin-T based realization of Fig. 1(a) with a floating switching capacitor. (b) PSpice simulation of the V_{C_1}–V_C trajectory. (c) X–W projection obtained by numerically integrating (7).

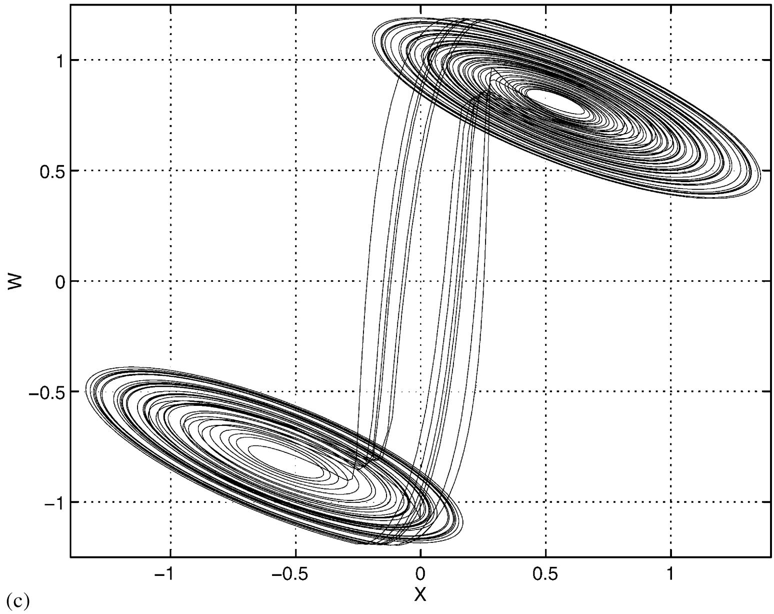

(c)

Fig. 4. (*continued*).

$$C_3 \dot{V}_{C_3} = -C_2 \dot{V}_{C_2} - \frac{K(V_{C_1} + V_{C_2}) + V_{C_3}}{R_1} - I_N, \tag{6c}$$

$$C\dot{V}_C = -I_N - \frac{V_C}{R}, \tag{6d}$$

where I_N is as given by (2) with $V_N = K(V_{C_1} + V_{C_2}) + V_{C_3} + V_C$.

A PSpice simulation of the V_{C_1}–V_C double-scroll is shown in Fig. 4(b); this was performed using Chua's diode of Fig. 1(c) and taking: $R_0 = 1$ kΩ, $C_0 = 5$ nF, $R_A = 10$ kΩ, $R_B = 500$ Ω, $R = 1.7$ kΩ, $C = 50$ pF, $R_4 = R_5 = 22$ kΩ, $R_6 = 3.3$ kΩ and $R_7 = 1.2$ kΩ. Note that K was increased slightly above unity to 1.05 in this case.

With the same settings used for the Wien-based oscillators and with $Z = V_{C3}/V_{BP}$, $W = V_C/V_{BP}$, the dimensionless form of (6) becomes

$$\dot{X} = 3(K-1)X + (3K-1)Y + Z, \tag{7a}$$

$$\dot{Y} = (K-1)(X+Y) + Z, \tag{7b}$$

$$-2\dot{Z} = (2K-1)(X+Y) + 2Z + f(V), \tag{7c}$$

$$-\varepsilon_c \dot{W} = \varepsilon_r W + f(V), \tag{7d}$$

where $f(V)$ has the same form as $f(Z)$ in (3d) with $V = K(X+Y) + Z + W$.

Numerical integration of (7) was performed with $K = 1.04$, $\varepsilon_r = \frac{2}{3}$, $\varepsilon_c = 0.04$, $\alpha_1 = 0.8$ and $\alpha_2 = -0.8$. The X–W projection is shown in Fig. 4(c).

A clear advantage of this Twin-T-based implementation is its use of a unity-gain amplifier. This feature permits the amplifier to reach its maximum bandwidth, thereby rendering the oscillator suitable for relatively high-frequency operation. It should be clear from Fig. 4(a) that there are two other nodes in the Twin-T network to which coupling can be made. Thus, with two possible positions for the switching capacitor and three internal Twin-T nodes, six possible combinations can realize the configuration of Fig. 1(a). Results similar to those shown in Fig. 4(b) and (c) are observed in all cases.

It is worth noting that, from a practical point of view, tuning a chaotic oscillator should not be achieved through any of the nonlinear resistor's parameters. In fact, these parameters should be fixed. Recalling the settings used to derive Eqs. (3), this implies that α_1 and α_2 should be constants. Hence, the sinusoidal oscillator's time-constant resistor R_0 should also be fixed. The center frequency of oscillation can then be adjusted by varying C_0. Since the absolute values of the coupling resistor R and the switching capacitor C are determined through the ratios ε_r and ε_c, respectively, we recommend that small values be chosen for R_0. This ensures a practical value of R and permits relatively high-frequency operation with sufficiently large values of C_0.

3. Estimating the frequency of oscillation

When the signal produced by a chaotic oscillator is nearly sinusoidal, the output power is concentrated in a single-frequency component centered near the operating frequency of the core sinusoidal oscillator (ω_{osc}). As the circuit is perturbed towards its chaotic region of operation, the power is spread to more frequency components both higher and lower than the center frequency of oscillation. The linearized form of Chua's circuit (see Fig. 2(a)) is given by $s^3 + a_2 s^2 + a_1 s + a_0 = 0$ where $a_2 = 1/RC_1 + (1 + RG_i)/RC$, $a_1 = 1/LC_1 + G_i/RCC_1$ and $a_0 = (1 + RG_i)/LC_1 RC$. In the inner segment of the nonlinearity $G_i = G_a$, while in the outer segments $G_i = G_b$. Hence, the estimated frequency range covered by the spectrum of the generated signal is given by

$$\omega_0 = \sqrt{a_1} = \frac{1}{\sqrt{LC_1}}\sqrt{1 + \frac{LG_i}{RC}}. \tag{8}$$

Consider replacing the inductor with its active RC emulation. In this case we can write $L = R_0^2 C_0$, where R_0 and C_0 are chosen arbitrarily. By selecting $C_0 = C_1$, (8) can be written in the form

$$\omega_0 = \omega_{osc}\sqrt{1 + \beta_i \frac{\varepsilon_r}{\varepsilon_c}}, \quad i = 1, 2, \tag{9}$$

where $\beta_1 = \alpha_1 = G_b R_0$, $\beta_2 = \alpha_1 + 2\alpha_2 = G_a R_0$ and $\omega_{osc} = 1/R_0 C_0$ (recall Eqs. (3), (5) and (7)). The frequency range covered by the spectrum of the generated signal from an RC implementation of Chua's circuit can be estimated using (9).

4. Experimental results

The chaotic oscillator shown in Fig. 2(b) was constructed using the AD844 CFOA and the AD713 VOAs. Capacitors C_1 and C_2 were set to 39 nF, R is 1.56 kΩ, R_B is a 5 kΩ pot. for tuning, and the rest of the components are as in the PSpice simulations. At $R_B = 3.15$ kΩ, a simple limit cycle either in the lower or the upper scrolls is born. When R_B is increased (the gain K is increased), a period-doubling sequence starts and a single scroll is formed. The upper and lower single scrolls are shown in Fig. 5(a) and (b), respectively. A further increase of R_B results in the birth of the double-scroll shown in Fig. 5(c).

Similar results were observed when a 10 pF switching capacitor was used in the two possible positions. The oscilloscope photographs in Fig. 5 show the V_{C_2}–V_C (Y–Z) projection where these two capacitors are grounded. The power spectrum of the voltage across C_2 is also shown in Fig. 5(d), spreading around a center frequency of 20.2 kHz. We note that the center frequency of the limit cycle is 20.5 kHz. As K is increased, this frequency shifts slightly to 20.2 kHz where the period doubling cascade

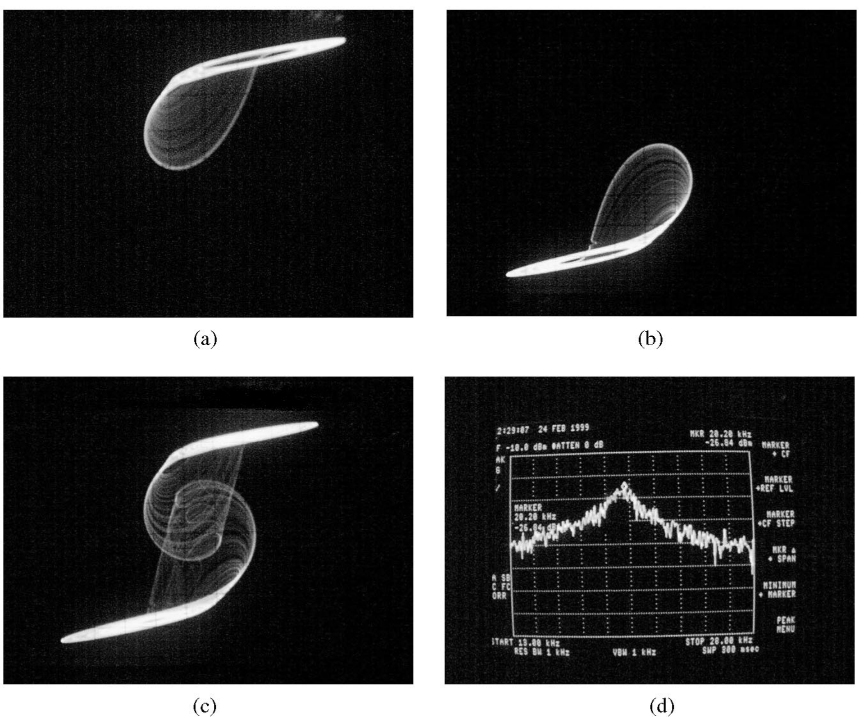

Fig. 5. Experimental results of Fig. 2(b) representing: (a) upper single scroll, (b) lower single scroll, (c) double-scroll attractor; Xaxis: V_{C_2} (1V/div) Yaxis: V_C (0.2V/div), (d) spectrum of V_{C_2} extending from 13 kHz up to 28 kHz.

starts. Using (9) to estimate the frequency range indicates a lower bound of $0.67\omega_{osc}$ (13.74 kHz) and an upper bound of $1.8\omega_{osc}$ (36.9 kHz).

5. Conjecture and concluding remarks

We have demonstrated here that the chaotic behavior of Chua's circuit can be preserved when it is physically decomposed into two separate blocks: a sinusoidal oscillator and a voltage-controlled nonlinear resistor. This decomposition also applies to Saito's chaotic oscillator (which is simply a classical $LC - R$ sinusoidal oscillator coupled to a hysteresis current-controlled nonlinear resistor [11]), the Colpitts oscillator [12], and all the chaotic oscillators reported in [13–18]. Therefore, we believe that there is sufficient evidence to state the following conjecture:

There exists a core sinusoidal or relaxation oscillator in any analogue autonomous chaotic oscillator which is capable of exhibiting simple limit cycle behavior. Accordingly, at least one chaotic oscillator can be derived from any sinusoidal or relaxation oscillator. The derivation process requires a nonlinearity which is not necessarily active.

Several remarks should be noted:

1. Although we (as well as others) have provided a large number of examples that support the above conjecture, there is as yet no general proof for it. This is due to the fact that there is as yet no set of necessary and sufficient conditions for chaos generation. However, for particular chaotic systems, we can prove the above conjecture by identifying the differential equations which describe a sinusoidal oscillator within the governing equations of the chaotic oscillator and by showing that the condition for oscillation is satisfied. This can be considered as proof of sufficiency since it requires knowledge of the chaotic system in advance. We have shown examples of such a proof in this work and in [11]. Furthermore, in [22], we have proposed generic circuit-independent realizations of Chua's circuit based on the simplest possible abstract models of RC sinusoidal oscillators where we require only that the basic formulae for the condition for oscillation and the frequency of oscillation are satisfied. Since in all cases the double-scroll dynamics have been preserved, we consider our conjecture proven in the particular case of Chua's circuit.
2. The conjecture provides a basis for describing a design process for chaotic oscillators. This process starts by designing a sinusoidal or relaxation oscillator that satisfies any set of circuit-design constraints and is then modified for chaos. The resulting chaotic oscillator can automatically inherit the features of the core oscillator if the design rules proposed in [19,20] are followed.
3. Since sinusoidal (relaxation) oscillators are active circuits, chaotic behavior can be expected from these oscillators when they are modified using *passive* nonlinear devices. As long as there are no specific features which only active nonlinear devices can fulfill, the use of simple passive nonlinear devices is strongly recommended.
4. The procedure for making second-order sinusoidal oscillators behave chaotically requires, in general, the addition of an extra energy storage element (inductor or

capacitor) and a nonlinear device to the oscillator's structure. However, there are two cases where no additional energy storage element is required. The first case is when the sinusoidal oscillator is already third order [12,16], while the second case is when a hysteresis-type nonlinear device is used [11,23]. On the other hand, modification of relaxation oscillators does not require any additional nonlinear devices since these oscillators are usually based on hysteresis nonlinear resistors. In fact, we expect that a third-order relaxation oscillator will most likely exhibit chaos for some sets of parameters with no need for any additional components.
5. The core sinusoidal (relaxation) oscillator in existing chaotic oscillators is reason for their limited spread spectrum bandwidth.
6. An example of a fourth-order chaotic oscillator based on the Twin-T network has been given in Section 2.3. An example of a fifth-order chaotic oscillator has also been reported in [24] based on a three-phase oscillator. These examples suggest that a class of higher-order (greater than three) chaotic oscillators can be designed based on a sinusoidal (relaxation) oscillator of order greater than two. Moreover, the coupling of multiple sinusoidal oscillators via passive nonlinear devices can also result in higher-order chaos [25].
7. In the case of chaotic signals produced by means of an analog phase-locked-loop (PLL), a voltage-controlled sinusoidal oscillator (VCO) serves as the core engine.

Acknowledgements

The AD844 and AD713 amplifiers used in this work were provided by Analog Devices. This work has been sponsored by the Enterprise Ireland Basic Research Program under grant number SC/98/740.

References

[1] M.P. Kennedy, L.O. Chua, Van der Pol and chaos, IEEE Trans. Circuits Systems—I 33 (1986) 974–980.
[2] R. Tokunaga, M. Komuro, T. Matsumoto, L.O. Chua, Lorenz attractor from an electrical circuit with uncoupled continuous piecewise-linear resistor, Int. J. Circuit Theory Appl. 17 (1989) 71–85.
[3] A. Namajunas, K. Pyragas, A. Tamasevicius, An electronic analog of Mackey-Glass system, Phys. Lett. A 201 (1995) 43–46.
[4] R.N. Madan, Chua's Circuit: A Paradigm for Chaos, World Scientific, Singapore, 1993.
[5] L.O. Chua, G. Lin, Canonical realization of Chua's circuit family, IEEE Trans. Circuits Systems—I 37 (1990) 885–902.
[6] T. Saito, S. Nakagawa, Chaos from a hysteresis and switched circuit, Philos. Trans. Roy. Soc. 353 (1995) 47–57.
[7] M.P. Kennedy, Robust op amp realization of Chua's circuit, Frequenz 46 (1992) 66–80.
[8] J.M. Cruz, L.O. Chua, An IC chip of Chua's circuit, IEEE Trans. Circuits Systems—II 40 (1993) 614–625.
[9] A. Rodriguez-Vazquez, M. Delgado-Restituto, CMOS design of chaotic oscillators using state variables: a monolithic Chua's circuit, IEEE Trans. Circuits Systems—II 40 (1993) 596–613.
[10] R. Senani, S.S. Gupta, Implementation of Chua's chaotic circuit using current feedback op amps, Electron. Lett. 34 (1998) 829–830.

[11] A.S. Elwakil, M.P. Kennedy, Chaotic oscillators derived from Saito's double-screw hysteresis oscillator, IEICE Trans. Fund. E82 (1999) 1769–1775.

[12] M.P. Kennedy, Chaos in the Colpitts oscillator, IEEE Trans. Circuits Systems—I 41 (1994) 771–774.

[13] O. Morgul, Wien bridge based RC chaos generator, Electron. Lett. 31 (1995) 2058–2059.

[14] A. Namajunas, A. Tamasevicius, Modified Wien-bridge oscillator for chaos, Electron. Lett. 31 (1995) 335–336.

[15] A.S. Elwakil, A.M. Soliman, A family of Wien-type oscillators modified for chaos, Int. J. Circuit Theory Appl. 25 (1997) 561–579.

[16] A.S. Elwakil, A.M. Soliman, Two Twin-T based op amp oscillators modified for chaos, J. Franklin Institute 335B (1998) 771–787.

[17] A.S. Elwakil, M.P. Kennedy, High frequency Wien-type chaotic oscillator, Electron. Lett. 34 (1998) 1161–1162.

[18] A.S. Elwakil, M.P. Kennedy, A family of Colpitts-like chaotic oscillators, J. Franklin Institute 336 (1999) 687–700.

[19] A.S. Elwakil, M.P. Kennedy, Towards a methodology for designing autonomous chaotic oscillators, Proceedings of the Sixth International Specialist Workshop on Nonlinear Dynamics of Electronic Systems NDES'98, Budapest, 1998, pp. 79–82.

[20] A.S. Elwakil, M.P. Kennedy, A semi-systematic procedure for producing chaos from sinusoidal oscillators using diode-inductor and FET-capacitor composites, IEEE Trans. Circuits Systems—I, in press.

[21] L.O. Chua, P.M. Lin, Computer-Aided Analysis of Electronic Circuits: Algorithms and Computational Techniques, Prentice-Hall, Englewood Cliffs, NJ, 1975.

[22] A.S. Elwakil, M.P. Kennedy, Generic RC realizations of Chua's circuit, Int. J. Bifurcation Chaos, in press.

[23] A.S. Elwakil, M.P. Kennedy, Systematic realization of a class of hysteresis RC chaotic oscillators, Int. J. Circuit Theory Appl., in press.

[24] A.S. Elwakil, M.P. Kennedy, Three-phase oscillator modified for chaos, Microelectron. J. 30 (1999) 863–867.

[25] A.S. Elwakil, M.P. Kennedy, Inductorless hyperchaos generator, Microelectron. J. 30 (1999) 739–743.